ACS APPLIED MATERIALS & INTERFACES

Research Article

www.acsami.org

# Design of Triple-Shape Memory Polyurethane with Photo-cross-linking of Cinnamon Groups

Lin Wang, Xifeng Yang, Hongmei Chen, Tao Gong, Wenbing Li, Guang Yang, and Shaobing Zhou*

Key Laboratory of Advanced Technologies of Materials, Ministry of Education, School of Materials Science and Engineering, Southwest Jiaotong University, Chengdu 610031, P.R. China

Supporting Information

**ABSTRACT:** A triple-shape memory polyurethane (TSMPU) with poly($\varepsilon$-caprolactone) -diols (PCL-diols) as the soft segments and diphenyl methane diisocyanate (MDI), N,N-bis (2-hydroxyethyl) cinnamamide (BHECA) as the hard segments was synthesized via simple photo-crosslinking of cinnamon groups irradiated under $\lambda$ > 280 nm ultraviolet (UV) light. Fourier transform infrared spectroscopy (FT-IR), proton nuclear magnetic resonance ($^1$H-NMR) and ultraviolet-visible absorption spectrum (UV−vis) confirmed the chemical structure of the material. Differential scanning calorimetry (DSC) and dynamic mechanical analysis (DMA) results demonstrated that the photo-crosslinked polymer possessed two transition temperatures, one is due to the melting point of the soft segment PCL-diols, and the other is due to the glass transition temperature. All these contributed to the cross-linked structure of the hard segments and resulted in an excellent triple-shape memory effect. Alamar blue assay showed that the material has good non-cytotoxicity and can be potentially used in biomaterial devices.

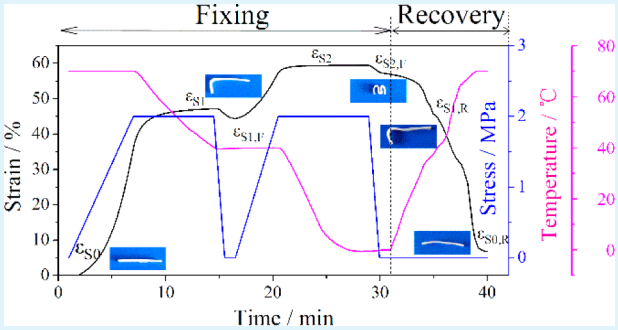


**KEYWORDS:** *triple shape memory, polyurethane, photo crosslink, cinnamate group*

## INTRODUCTION

Shape memory polymers (SMPs), as an emerging class of intelligent materials, are able to deform and fix into a temporary shape, and then recover to their initial shape[1,2] responding to an environmental stimulus, for instance, thermal,[3−6] light,[7,8] electro,[9] magnetic field,[10] or solvent.[11] Among these elements, thermally induced SMPs are widely investigated. On the basis of different switching segments, SMPs can be commonly classified into the following two categories: one is $T_m$-type SMPs which has a crystalline segment, and the other is $T_g$-type SMPs which contains amorphous segment.[12] Up to now, SMPs have obtained increasing interest due to their potentially abundant applications as biomedical materials.[13,14] Besides, shape memory polyurethane (SMPU) also has a wide range of applications in the biomedical field.[15,16] For example, using the shape memory effect of polyurethane based on poly($\varepsilon$-caprolactone) (PCLU), Li[15] prepared fast self-expandable stents which could be used in tissue engineering. Betz reported available commercially polyetherurethanes (PEU) which is used in artificial hearts and pacemaker leads. [16]

Recently, triple shape memory polymers (TSMPs) have attracted more and more attention.[17] In contrast to the classical SMPs which have only one temporary shape and thus exhibit dual-shape effect, TSMPs could remember two temporary shapes. Generally, TSMPs include either the multiphase polymer networks which have obvious differences between transition temperatures,[18−20] or the polymers with a wide range of temperature changes.[21,22] To date, TSMPs have been widely applied in intelligent medical devices, assembling systems, and minimally invasive surgery.[18,23] However, in the face of ever-increasing complex demands on the use of intelligent medical devices, TSMPs can be used under two transition temperatures which provide more flexible application in intelligent medical devices compared to the traditional SMPs with only one particular transition temperature. Among them, the vascular application has received considerable attention. For example, Lendlein reported that crosslinked poly($\varepsilon$-caprolactone), which contained polyethylene glycol (PEG) as side chains (CLEG), could be inserted into the body as a removable stent used a compressed shape A, and when placed at a requisite position, the stent could be recovered to shape B, lastly it could contracted to shape C under the external stimulus for easy to remove.[24] Furthermore, future desired SMP devices will require multifunction, which includes multi-stimuli shape memory, triple shape memory, two-way SMP, and more.[25]

SMPU based on poly($\varepsilon$-caprolactone) (PCL) is a representative SMP. PCL is well-known for its biodegradability in biomedical applications.[26] SMPU was often investigated for the application as biomaterials. For example, Lendlein[27] and Lee[28] synthesized SMPU based on PCL and predicted their potential applications in medical devices due to their excellent biodegradability and biocompatibility. In addition, SMPU has

Received: May 31, 2013
Accepted: September 30, 2013
Published: September 30, 2013

  

other special properties. It possesses a tunable shape recovery temperatures,[29] and good processing ability.[30] SMPU contains the hard segments and the soft segments, the soft segments mostly including crystalline polyethers or polyesters whose melting temperature ($T_m$) is used as the shape recovery temperature.[31]

In this study, we designed a new triple shape memory system which contains both a $T_m$-type segment and a $T_g$-type segment, differing from the previously reported triple shape memory polymers which have either two $T_m$-type segments or two $T_g$-type segments. Firstly, shape memory polyurethane based on PCL with pendant cinnamon groups was synthesized. Then, the resultant polymer (PCLU) was photo-crosslinked by an UV light irradiation to obtain the triple shape memory polyurethane (TSMPU). The cinnamon groups with good photosensitivity were often applied to synthesize photo-induced shape memory polymers.[32] The double bond in the cinnamon group can occur [2+2] cycloaddition reaction under the $\lambda > 280$ nm UV light irradiation to form a four-membered ring, whereas the photo-crosslinking structure can be cleaved to form the double bond by the irradiation of the $\lambda < 280$ nm UV light.[7] Thus, the specific light reversible nature can be reflected in the polymer, which is expressed as deformation and recovery of the polymer. However, different from the mechanism of photo-responsive shape memory polymer, in this system we find that the polymer has two transition temperatures, one for the melting point of PCL-diols from the polyurethane soft segments, the other for the glass transition temperature of the crosslinking structure of polyurethane hard segments which were obtained through the cycloaddition reaction of the cinnamon groups initiated by UV light, resulting in the thermally induced triple shape memory effect.

## EXPERIMENTS AND METHODS

**Materials.** Ethylene glycol (EG), $\varepsilon$-caprolactone ($\varepsilon$-CL), and stannous octoate [$Sn(Oct)_2$, 95%] were purchased from Aldrich. Stannous chloride ($SnCl_2$), diethanolamine (DEA), cinnamate, and N,N-dimethyl formamide (DMF) were purchased from Kelong chemical reagent factory in Chengdu (China). MDI was purchased from Tokyo Chemical Industry Co. LTD. $\varepsilon$-CL, EG, DEA, and DMF were dried over calcium hydride to remove water and distilled under a reduced pressure. Cinnamate was recrystallized before use. The cytotoxicity assays was determined with osteoblasts.

The synthesis of PCL-diols (HO-PCL-OH). PCL-diols was synthesized through a typical ring opening polymerization according to our previously report[33] (Scheme 1A). In brief, $\varepsilon$-CL (10 g, 87.7 mmol), EG (0.155 g, 2.51 mmol), and $SnCl_2$ (0.05 g) were added into a 50 mL bottom flask with a stopcock. Then, the reaction device was vacuumized for 3 h, and lastly, the reaction system was polymerized at 140 °C for 6 h. The purification process of obtained polymer as follows. The polymer was sequentially dissolved in dichloromethane, the solution precipitated into ethanol, and the precipitate dried under vacuum at room temperature for 24 h; 9.15 g (91.5%, yield) PCL-diols was obtained.

**Preparation of BHECA.** BHECA was synthesized through an ammonolysis reaction as displayed in Scheme 1B. Firstly, methyl cinnamate was synthesized from methanol and cinnamate via esterification. After that, BHECA was synthesized from methyl cinnamate re-crystallized in ethanol and DEA via the ammonolysis reaction.[34] The typical synthetic route was as follows. Methyl cinnamate (4.86 g, 0.03 mol), sodium methylate (0.029 g), and DEA (6.31 g, 0.06 mol) were added into a 100 mL flask and heated to 120 °C under stirring, then the reaction device was conducted under reduced pressure. After reaction for 2 h, a yellow-green viscous liquid was obtained. BHECA was separated from the mixed liquid via precipitation with 150 mL of ice water and hydrochloric acid mixed

**Scheme 1. Synthetic Route of (A) PCL-Diols, (B) BHECA, (C) Photosensitive PCLU with Pendent Cinnamon Groups, and (D) TSMPU Prepared by UV Light Crosslink with a 365 nm Wavelength.**

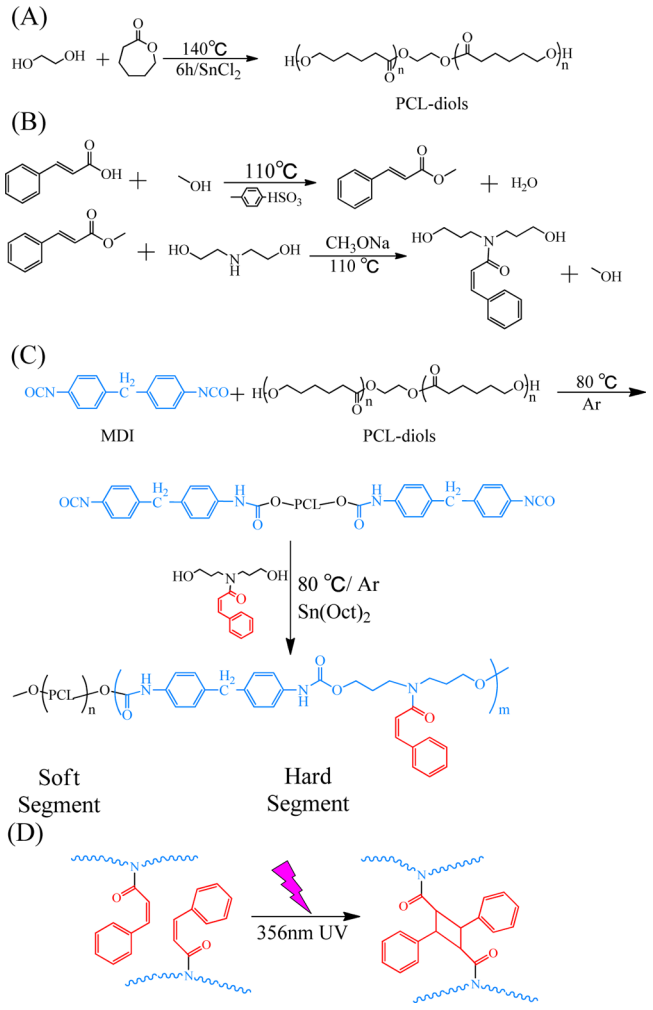


liquid. Finally, a type of white solid was obtained via recrystallization in ethyl acetate.[35] The product was further purified with column chromatography using 1:1 dichloromethane/petroleum ether as eluent. Lastly, the white solid was obtained, and further dried under vacuum for 24 h; 4.15 g BHECA was obtained (85.3%, yield).

**Preparation of PCLU.** PCLU was prepared by a solution copolymerization at the temperature of 85 °C in DMF. A series of photoinduced PCLU were synthesized with the typical two-step ways as displayed in Scheme 1C. Taking the PCLU with MDI:BHECA:PCL-diols ratio of 5:4:1 as an example, firstly PCL-diols (2.00 g, 0.541 mmol) was added into a 100 mL three-necked round flask equipped with magnetic stirrer and dewatered at 80 °C for 3 h under vacuum to remove the moisture, then MDI (0.676 g, 2.705 mmol) was quickly added into the three-necked round flask which was connected to the backflow device and an Ar gas protection device. The reaction system was conducted at 80 °C for 2 h with continuous stirring in the presence of Ar gas. After 2 h, preweighed BHECA was dissolved in DMF and added dropwise into the reaction system with $Sn(Oct)_2$ as the catalyst, the reaction carried out at 80 °C for 5 h. Finally, pale yellow viscous liquid was obtained, and precipitated in hexane. White solid was obtained and further dried under vacuum at room temperature for 48 h.

**Preparation of TSMPU.** 2g PCLU was dissolved in 20 mL of DMF, and the PCLU solution was irradiated by a 100 W UV light with a 365 nm wavelength as shown in Scheme 1D. Irradiation distance was kept at 10 cm and irradiation time was kept for 10 min. The photo-

crosslinked PCLU solution was poured into a PTFE plate (2 cm × 2 cm) and kept at 65 °C for 24 h to remove most of DMF. After that the film was further dried under vacuum for 48 h. Finally, TSMPU films with a thickness of 1.1 mm were prepared for DMA, mechanical tensile test and shape memory tests.

**Characterization Methods.** FT-IR was recorded on a Nicolet 5700 IR spectrometer. All samples were obtained by KBr plates in which dry polymer power was blended with KBr at a weight ratio of 0.5-1%. $^1$H NMR spectra were obtained with a Bruker AM-300 spectrometer. Tetramethylsilane (TMS) was used as the internal standard and $CDCl_3$ was used as solvent. The UV spectra were recorded on a ultraviolet−visible (UV−vis) spectrophotometer (UV-2550, Shimadzu, Japan) in the wavelength range of 200−400 nm. The degree of photo crosslinking could be calculated by determining the intensity changes of the absorption peak at 280 nm. The typical process is discussed as below: first, PCLU polymer/DMF solution with predetermined concentration was prepared; second, the polymer solution was irradiated under 365 nm UV light for 1, 5, and 10 min, respectively, and 2 mL of polymer solution was pipetted at each time point; then the changes of absorption intensity at 280 nm was determined by UV−vis spectrophotometer. Thermal properties of polymers were determined by DSC (TA DSC-Q100). To eliminate any unknown thermal history of the samples, we repeated heating and cooling from −10 °C to 100 °C, then the DSC curves of the second heating and cooling process were obtained. Both the heating and cooling ratio was 10 °C min$^{-1}$. All data were used from the second heating and cooling process. DMA was measured using a specimen with size of 12 × 4 × 1 mm$^3$ (length × width × thickness) carried out with a DMA (TA DMA-Q 800) at heating ratio of 3 °C min$^{-1}$ from -20 to 120 °C and at a frequency of 1 Hz. The storage modulus E′ was tested. The static tensile tests were performed with a Universal testing machine instron 5567 (Instron Co., Massachusetts) under speed of 1 mm min$^{-1}$ at room temperature. Gel permeation chromatography (GPC) was carried out with a Water 2695 separation module equipped with a StyragelHT4DMF column calibrated with polystyrene narrow standards operated at 40% and series 2414 refractive index detector. Atomic Force Microscope (AFM) (CSPM5000, Being, China) was used to characterize the surface morphology of PCLU and TSMPU films, which operated in tapping mode. The cross-sections of PCLU and TSMPU films with freeze-fracture were observed using a Quanta200 Scanning Electron Microscope (SEM, FEI, America).The accelerating voltage was 20 kV Gel fraction and swelling experiment were carried out. Dried TSMPUs ($m_0$) were immersed in DMF. The specimens were taken out after 24h ($m_1$) and dried under vacuum at room temperature for 24 h, and record the weight ($m_2$) of obtained dried specimens. The gel fraction ($Q_g$) and the degree of swelling ($Q_s$) were calculated according to the following equations

$$Q_g = \frac{m_2}{m_0} \times 100\% \quad (1)$$

$$Q_s = \frac{m_1}{m_0} \times 100\% \quad (2)$$

**Investigation of the Triple Shape Memory Effect.** The triple shape memory properties were measured by using strip specimens of the photo-crosslinked polymer. The strip was heated at 70 °C for 1 min, and was bended to an "L" shape, named as temporary shape I. Then, the shape I specimen was moved to a 40 °C warm water for fixing deformed shape for 1 min. After that, the shape I specimen was bended to an "M" shape, named as shape II. And the shape II specimen was moved to a 0 °C ice water for fixing deformed shape for 1 min. When the shape II specimen was induced with 40 °C warm water, it could be observed that shape I specimen could be obtained. And then the specimen was placed in 70 °C water, the original shape could be obtained.

Shape memory fixity ratio and recovery ratio were measured using strip shaped specimens carried out on a DMA (TA, DMA-Q 800), using a controlled force mode according to our designed experiment. A typical testing procedure was performed as previous report.[24] Firstly, straining the specimen (shape 0) at a stress rate of 0.5 MPa /min to 2 MPa, a temporary shape I at 70 °C was obtained, marked as $\varepsilon_{SI\text{-}F}$ ; and then cooled to 40 °C and released the stress, marked as $\varepsilon_{SI}$; Secondly, straining the specimen of shape I at a same stress rate to obtain another temporary shape II, marked as $\varepsilon_{SII\text{-}F}$, and then cooled to 0 °C and released the stress, marked as $\varepsilon_{SII}$. Finally, the temporary shape II was heated in 40 °C, the strain marked as $\varepsilon_{SI,R}$, and the specimen was heated to 70 °C, the strain marked as $\varepsilon_{S0,R}$. The shape memory fixity ratio and recovery ratio were calculated according to the following equations

$$R_f(0 \rightarrow I) = \frac{\varepsilon_{SI}}{\varepsilon_{SI-F}} \times 100\% \quad (3)$$

$$R_f(I \rightarrow II) = \left(1 - \frac{\varepsilon_{SII-F} - \varepsilon_{SII}}{\varepsilon_{SII-F} - \varepsilon_{SI}}\right) \times 100\% \quad (4)$$

$$R_r(II \rightarrow I) = \frac{\varepsilon_{SII-F} - \varepsilon_{SII}}{\varepsilon_{SII-F} - \varepsilon_{SI}} \times 100\% \quad (5)$$

$$R_r(I \rightarrow 0) = \left(1 - \frac{\varepsilon_{S0,R}}{\varepsilon_{SI}}\right) \times 100\% \quad (6)$$

**In Vitro Cytotoxicity Assays.** Samples, cut into small round flakes (about 12 mm in diameter), were sterilized by immersing in ethanol (75 wt%) and ultraviolet irradiation for 60 min before cultured with osteoblasts in vitro. Osteoblasts were grown in α-modified essential medium (α-MEM) (HyClone, USA) with 10% fetal bovine serum (FBS). The cells with a density of 1 × 10$^4$ cells/well were seeded onto the samples in 24-well plate (Sigma) and maintained at 37 °C in a humidfied incubator with 5% $CO_2$. At the preset time points of 1, 3, and 5 days, Alamar blue assay was performed to evaluate the cytotoxicity of materials as previously reported.[36] The medium was removed and 300 μL of Alamar blue solution (10% Alamar blue, 80% media 199 (Gibcos) and 10% FBS; v/v) was added into each well and incubated for further 3 h. Cells cultured in wells without materials were just as blank controls. After 3 h, 200 μL of reduced Alamar blue solution was transfer into a 96-well plate (Sigma) and read at 570 (excitation) / 600 (emission) in an ELISA microplate reader (Molecular Devices, Sunnyvale, CA). Cell morphology on the TSMPU films were detected by optical microscopy (ZEISS Axio Imager A1 m).

**Statistic Analysis.** Single factorial analysis of variance was performed to determine statistical significance of the data. The experiment repeated three times and the results were reported as mean ± standard deviation.[36]

## RESULTS AND DISCUSSION

**Characterization of TSMPU.** Generally, PCLU exhibit dual-shape memory effect because of the micro-phase separation structure constituted by the hard and soft segments. In addition, the cinnamon groups with good photoreversibility are nontoxic and can be metabolized in the body,[37] and they could be introduced into PCLU to synthesize photoinduced shape memory polymers. However, most interestingly, we found that the photo-cross-linked PCLU exhibits a temperature-responsive triple-shape memory effect in addition to the photo-responsive dual-shape memory effect.

The chemical structure of the PCLU was investigated. Figure 1A shows the FTIR spectra of the methyl cinnamate, BHECA and PCLU. Methyl cinnamate, BHECA, and PCLU exhibit characteristic absorptions of C═C bond at 1635, 1628, and 1628 cm$^{-1}$, respectively. In the spectrum of the BHECA, the peak at 1170 cm$^{-1}$ ascribed to the C-N stretching vibration appears compared to methyl cinnamate. And in the spectrum of the PCLU, the characteristic absorptions of PCL, BHECA, and urethane are all remained, such as the absorptions of C═O stretching vibration of PCL-diols at 1730 cm$^{-1}$, C═C

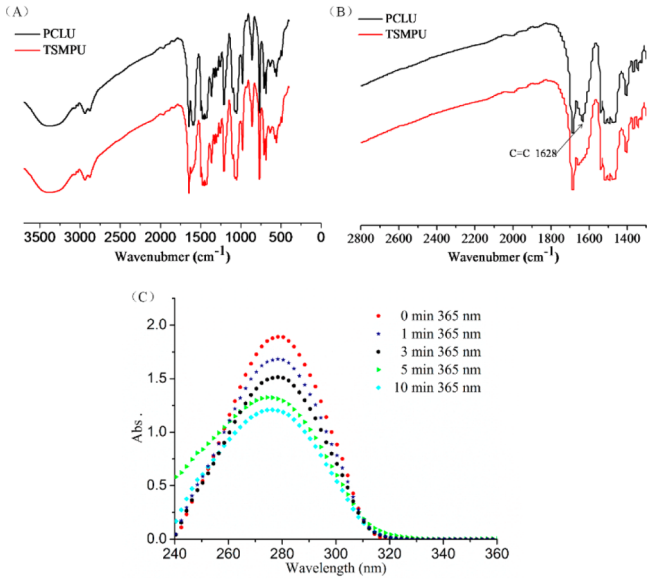


**Figure 1.** (A) FT-IR spectra of methyl cinnamate, BHECA, and PCLU, (B) $^1$H NMR spectrum of BHECA, PCL-diols, and PCLU.

stretching vibration at 1620 cm$^{-1}$ and C-N stretching vibration at 1170 cm$^{-1}$, respectively. The FTIR spectra shows that there is no residual MDI monomer. In the spectra of methyl cinnamate, BHECA and PCLU, the absorptions of C═C stretching vibration is blue shift. The reason is that during the formation of small molecules to macromolecules, the steric hindrance as well as the introduction of functional groups disturbed the intramolecular interactions. These results also indicate that PCLU was synthesized successfully.

To further validate the successful synthesis of the materials, the structure of methyl cinnamate (Figure S1 in the Supporting Information) and BHECA is confirmed by $^1$H NMR. In the $^1$H NMR spectrum (see Figure S1 in the Supporting Information) of methyl cinnamate, the chemical shift at 3.81 ppm (a) is attributed to the protons of methyl, and the presence of chemical shifts of −CH═CH− groups in cinnamon could be found at 6.49 ppm (b) and 7.69−7.65 ppm (c). The characteristic chemical shifts and the integrated area of distinct chemical shifts in $^1$H NMR spectrum confirmed that methyl cinnamate was synthesized successfully. In the $^1$H NMR spectrum of BHECA, the chemical shifts at 3.65 ppm (a), 3.87 ppm (b), 6.45−6.51 ppm (c), 7.69 ppm (e), and 7.50−7.35 ppm (d, f−g) are attributed to $-CH_2-N$, $-CH_2-O$, C═CH−CO, Ph−CH═C, and phenyl H atoms, respectively. In the $^1$H NMR spectrum of PCL-diols, PCL-diols exhibits chemical shifts of $CH_2$ at 4,24 ppm (h), 4.03 ppm (p), 3.62 ppm ($p_1$), 2.28 ppm (i), 1.62 ppm (j), and 1.36 ppm (k), suggesting a pure ester structure of PCL-diols.[15] From the intensity of signal $p$ and $p_1$, the number of repeating units ($n$) is established as 31.9, consequently, PCL-diols with $M_n$ of 3700 g/mol is calculated. In the $^1$H NMR spectrum of PCLU, most of the characteristic chemical shifts from PCL-diols are still remained; however, some new chemical shifts appeared. The chemical shifts of 7.45-761 ppm ($x$,$y$) are attributed to the protons in phenyl ring, the chemical shift of $-N-CH_2-$ at 3.75 appeared, and the chemical shifts of −CH═CH− group in cinnamon at 6.49 ppm (c) and 7.69−7.65 ppm (e) are emerged. The presence of these characteristic chemical shifts confirmed that PCLU containing cinnamon group was synthesized successfully. Furthermore, the actual ratios of PCL, MDI, and BHECA in the copolymer were calculated from the integrated area of distinct chemical shifts (from the intensity of signal p, r, and c, respectively.). All the resultant PCLU polymers have approximate ratios of monomer units to the feeding compositions, which are summarized in Table 1.

To confirm the formation of photo-crosslinked TSMPU, FTIR and UV-vis spectrophotometer are employed. Figure 2A shows the FT-IR spectra of PCLU and TSMPU. For PCLU the characteristic absorptions of C═C stretching vibration at 1628 cm$^{-1}$ can be found. After being irradiated by the $\lambda$ = 365 nm UV light, the absorption intensity of C═C stretching vibration decreases, as shown in Figure 2B. To further analyze the formation of the crosslinking network, PCLU samples were measured by UV-vis absorption spectrum in DMF solution. As

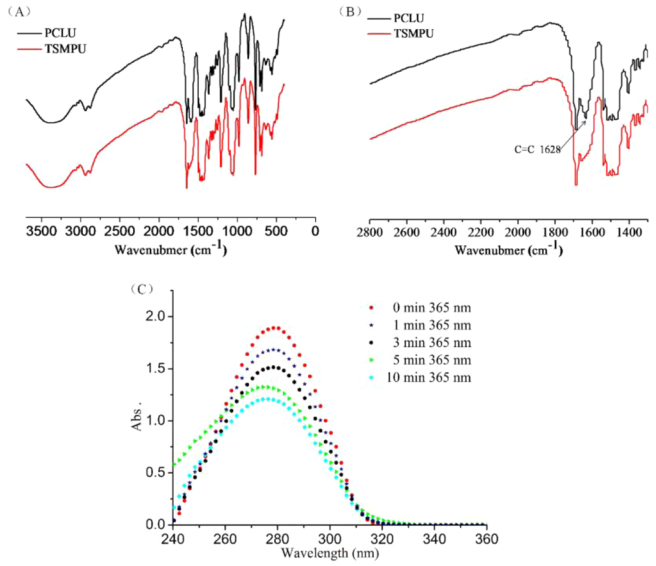


**Figure 2.** (A) FTIR spectra of PCLU and TSMPU; (B) local magnified image of FTIR spectra A; (C) UV−visible spectra of PCLU which are obtained by increasing the irradiation time with 365 nm UV wavelength.

**Table 1. Molal Ratio, Transition Temperature, and Molecular Weight Characterization of PCLU with Different Compositions**

| sample | MDI:BHECA:PCL (molal ratio)[a] | HS%[a] | MDI:BHECA:PCL (molal ratio)[b] | HS%[b] | $T_{trans}$ (°C) | Mn[c] (× 10$^{-4}$) | Mn[d] (× 10$^{-4}$) | $M_w/M_n$ |
|---|---|---|---|---|---|---|---|---|
| PCL-diols | | | | | 53.2 | 0.37 | 0.3657 | 1.22 |
| PCLU(3:2:1) | 3:2:1 | 24.77 | 2.95:1.98:0.97 | 25.87 | 34.4 | 6.875 | 7.298 | 1.57 |
| PCLU(5:4:1) | 5:4:1 | 37.14 | 4.91:3.97:0.94 | 34.33 | 36.1 | 6.330 | 6.754 | 2.32 |
| PCLU(8:7:1) | 8:7:1 | 49.58 | 7.88:6.92:0.96 | 50.29 | 40.1 | 5.287 | 5.549 | 2.46 |
| PCLU(10:9:1) | 10:9:1 | 52.26 | 9.72:8.87:0.85 | 58.89 | 44.1 | 5.893 | 6.089 | 2.73 |

[a]Molal composition in feed; [b]Molal composition determined by $^1$H-NMR; [c]Obtained by $^1$H-NMR; [d]Obtained by GPC.

**Table 2. Mechanical Properties, Gel Fraction, and Swelling Fraction of TSMPU**

| sample | tensile modulus (MPa) | crosslink density (mol $m^{-3}$) | maximum tensile strength % | $Q_g$ (%) | $Q_s$ (%) |
|---|---|---|---|---|---|
| TSMPU(3:2:1) | 5.01 ± 0.09 | 674.05 ± 12.11 | 372 ± 5 | 31.3 ± 0.4 | 122.4 ± 2.1 |
| TSMPU(5:4:1) | 6.42 ± 0.07 | 863.75 ± 9.42 | 367 ± 4 | 34.2 ± 0.6 | 145.4 ± 1.8 |
| TSMPU(8:7:1) | 7.26 ± 0.10 | 976.76 ± 13.45 | 335 ± 4 | 22.7 ± 1.2 | 103.5 ± 2.4 |

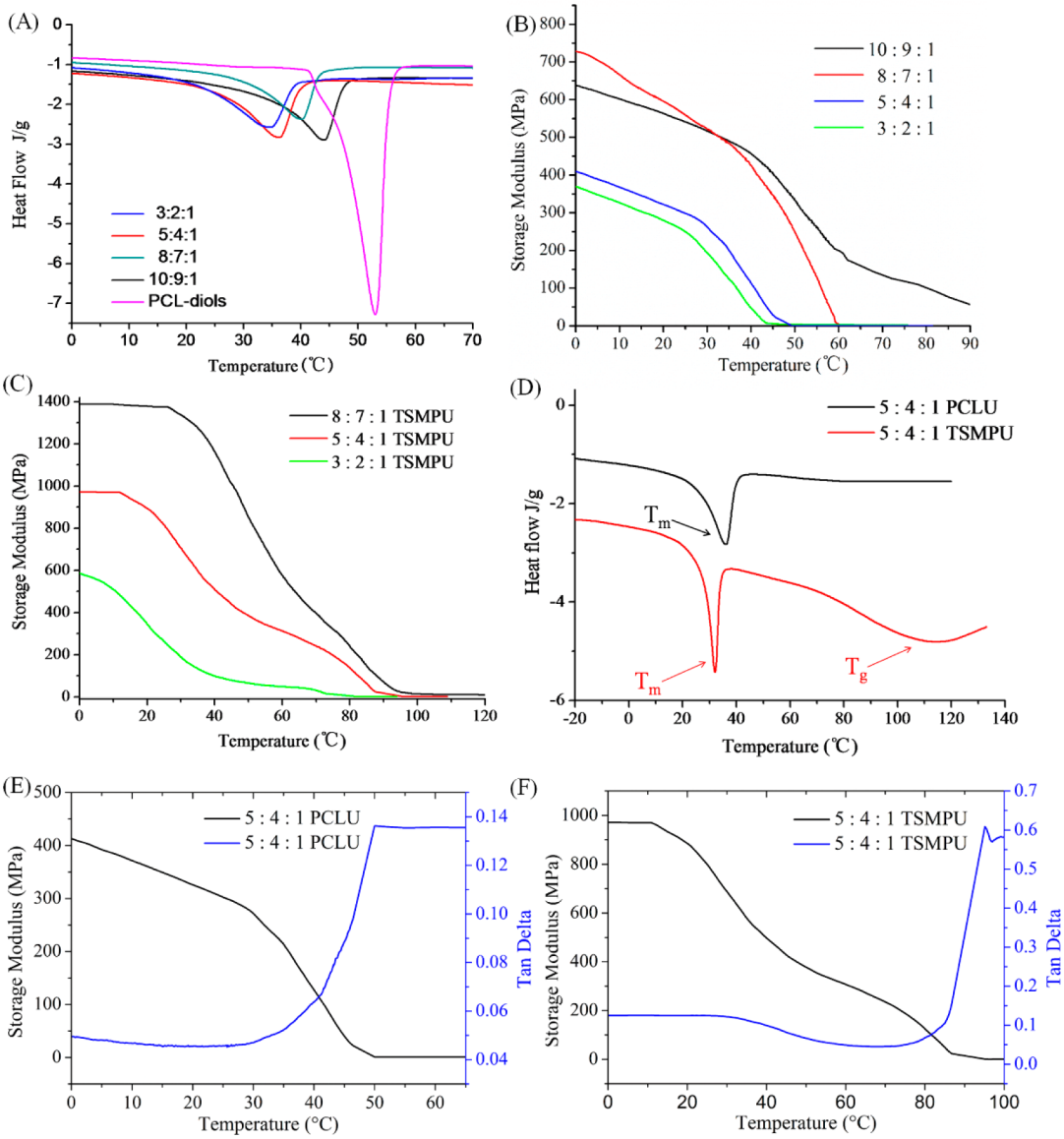


**Figure 3.** (A) DSC curves of PCLU with different ratio of hard segment and PCL-diols; (B) DMA curves of PCLU with different hard segment ratios; (C) DMA curves of TSMPU with different hard segment ratios; (D) DSC curves of PCLU and TSMPU with MDI: BHECA: PCL-diols ratio of 5:4:1; (E) DMA curves of PCLU and (F) TSMPU with MDI: BHECA: PCL-diols ratio of 5:4:1.

seen from Figure 2C, the cinnamon group shows a maximum absorption at 280 nm, the intensity of the absorption peak decreased with the increasing of irradiation time under the irradiation of 365 nm UV light. The UV−vis results indicate that the cinnamon groups underwent a [2+2] photo-cyclo-addition reaction. The conversion rate of double bond in the cinnamon group can be used as the degree of photo crosslinking.[32] The results further indicate that the TSMPU was prepared successfully.

In addition, from the result of UV−vis spectrum, the degree of photo-cross-linking could be calculated.[32] The degree of photo-cross-linking could reach to 34% when the irradiation time up to 10 min, which can endow the polymer good thermally induced shape memory effect. To confirm the crosslinked structure, $Q_g$ and $Q_s$ were obtained from the gel fraction and swelling experiment as shown in Table 2. From the results of the $Q_g$ and $Q_s$, TSMPU (8:7:1), TSMPU (5:4:1), and TSMPU (3:2:1) exhibit the gel fraction of 22.7, 34.2, and 31.3%, respectively. However, there is not gel obtained for TSMPU (10:9:1), which may be attributed to the reduced chain motion of the hard segment.

**Thermal Property of TSMPU.** To determine the transition temperature of the shape memory polymer, we tested DSC and DMA. On the basis of the structure, this system is different

from the tradition triple shape memory generally reported.[20,38,39] Here, we developed a new method to synthesize a triple shape memory system with an easy and controllable method. In this system, there is a wide temperature difference between the soft segment in the polyurethane and the photo-cross-linked structure from polyurethane hard segment, in which the $T_m$ of PCL-diols and the $T_g$ of the crosslinking structure of the hard segment can act as the two transition temperatures of the triple shape memory polyurethane. Figure 3A shows the DSC curves of four species of PCLU with possess four different ratios of the soft segments and hard segments. The soft segments mostly are crystalline polyethers or polyesters, whose melting temperature ($T_m$) is considered the shape recovery temperature. From Table 1 and DSC curves, we can find that the transition temperature ($T_{trans}$) of the polymer increases from 34.4 °C to 44.1 °C with the increase of hard segments content from 24.77% to 52.26%. In general, $T_{trans}$ of PCLU is lower than $T_m$ of PCL-diols. Additionally, PCLU exhibits micro-phase separation, and the degree of phase separation decreases with the content of hard segments increasing,[40] which causes the $T_m$ of soft segments to increase.[40,41] Figure 3B shows the DMA curves of PCLU with different hard segment contents. In contrast to these samples, we can find that the phase transition temperature increases from 35 °C to 37, 41, and 45 °C with the increasing of the hard segments content. From the DMA curves, it seems that the changes in storage modulus ($E'$) of all specimens become more obvious with the hard segments increasing. And below room temperature the storage modulus increases with the increasing of hard segments, owing to the reduced chain motion with higher hard segments and a high crystallinity of soft segment at lower temperature.[42] The continuous decrease in $E'$ until $T_m$ of soft segments, where a sharp decrease is observed, is related to the melting transition temperature of soft segment.[42] The SMPs with a higher storage modulus would possess a faster recovery ratio.[41]

From the above discussion of gel fraction, we can find that TSMPU (10:9:1) could not form the crosslinked structure under the UV irradiation, and thus it is not discussed under the below discussion. Interestingly, from the DMA curve in Figure 3C, it can be seen that all TSMPU with different ratios of the hard segments had two obvious regions of reduction in modulus, one for the $T_m$ region of PCL-diols from the soft segment of TSMPU, the other for the $T_g$ region of the crosslinking hard segment from the light dimerization of cinnamon groups. From the results of DSC and DMA, we can find that TSMPU (5:4:1) has a higher storage modulus than that of PCLU due to the photo-crosslinked structure. Moreover, it exhibits two obvious transition regions, suggesting that it possesses an excellent triple shape memory effect with the lower transition temperature near to the body temperature (37 °C). Thus, it was selected to perform the following investigations. Figure 3D shows the DSC curves of PCLU with MDI: BHECA: PCL-diols ratio of 5:4:1 before and after irradiated with UV light (TSMPU). From the DSC curves, we can clearly find that TSMPU has two distinct transition temperatures, one belongs to the $T_m$ transition region of the soft segments, the other is the $T_g$ transition region of the cross-linked hard segment. Moreover, the $T_m$ of PCL-diols decreases from 36.8 °C for PCLU to 32.4 °C for TSMPU, due to the fact that the photo-cross-linked network hinders the crystallization of PCL segments.[40] From the DMA curves in Figure 3E, F, we can also find that PCLU has only one transition temperature but TSMPU has two transition temperatures, which is similar to the results of DSC. The decrease in the storage modulus from 900 to 400 MPa lead to the first temperature transition, and the decrease of the modulus from approximate 300 to 0 MPa result in the second temperature transition. Compared to PCLU, TSMPU has a great increase in modulus due to the crosslinking structure. In Figure 3E, the storage modulus continues decreasing and a sharp decrease is observed with the temperature increasing from 35 to 50 °C, whereas the tan delta shows a sharp increase and a maximum value appears at 50 °C. However, in Figure 3F, there are two obviously continuous decreasing regions for the storage modulus. Moreover, there occur two maximum peaks of tan delta, one decreasing region in ∼30 °C isdue to the melting of soft segments, the other decrease region in ∼ 70 °C is due to the glass transition region of the cross-linked hard segments. The great difference of the $E'$ for the two transition regions indicates that the material has an excellent triple shape memory effect.[40] The two temperatures of 40 and 70 °C were selected as the low transition temperature and the high transition temperature, respectively.

**Thermal-Induced Triple Shape Memory Properties.** In the shape memory experiment, we chose the TSMPU sample with MDI: BHECA: PCL-diols ratio of 5:4:1 to study the triple shape memory effect. Firstly, quantitative demonstration of triple shape memory properties is shown in Figure 4A, where the stress-strain-temperature curves are obtained in strain mode from DMA testing. The $R_f$ and $R_r$ of the triple-shape memory cycles were calculated by the eqs 1−4. The $R_f$ (0 → I) and $R_f$ (I → II) reach to 94.39 and 84.73%, respectively. And the $R_r$ (II → I) and $R_r$ (I → 0) are 90.09% and 84.78%, respectively. Lastly, the triple-shape memory process of TSMPU is showed in Figure 4B and Movie S1. The species was deformed to temporary shape I at 70 °C. When the deformed shape I was kept in 40 °C, the temporary shape could be fixed unloaded, and could be kept very well, next the shape I was deformed to temporary shape II at 40 °C, and cooled in ice water to fix the shape. When the temporary shape II was placed in water at 40 °C for 15 s, it could return to the shape I, and it could return to initial shape when placed again in water at 70 °C for 2 s. All species were carried out for three times, both the shape fixity ratio and recovery ratio remain above 80%, which are summarized in Table S1 in the Supporting Information.

**Mechanism of Triple Shape Memory System.** There is always a micro-phase separation in polyurethanes, as shown in Figure S2 in the Supporting Information. Figure S2 in the Supporting Information shows that the PCLU and TSMPU present a phase-separated microstructure. In the AFM images (see Figure S2A, B in the Supporting Information), the light regions correspond to soft crystalline regions. Differently sized spherulites are observed for PCLU and TSMPU. The crosslinked structure in TSMPU prevent the crystallization and movement of soft segments.[42] The SEM micrographs of the PCLU and TSMPU in Figure S2C, D in the Supporting Information were taken from the cross-sections by freeze fracture, and a homogeneous matrix that contains a dispersed crystallites phase can be observed. There is a distinct difference between the PCLU and TSMPU. [43] PCLU is different from common polyurethane whose soft segments are highly crystalline at room temperature.[40] Different from the mechanism of thermal or photoinduced dual shape memory polyurethane, in our system, cinnamon groups are introduced into the hard segments, and can occur [2+2] cycloaddition under 365 nm UV light to form a network structure. The soft

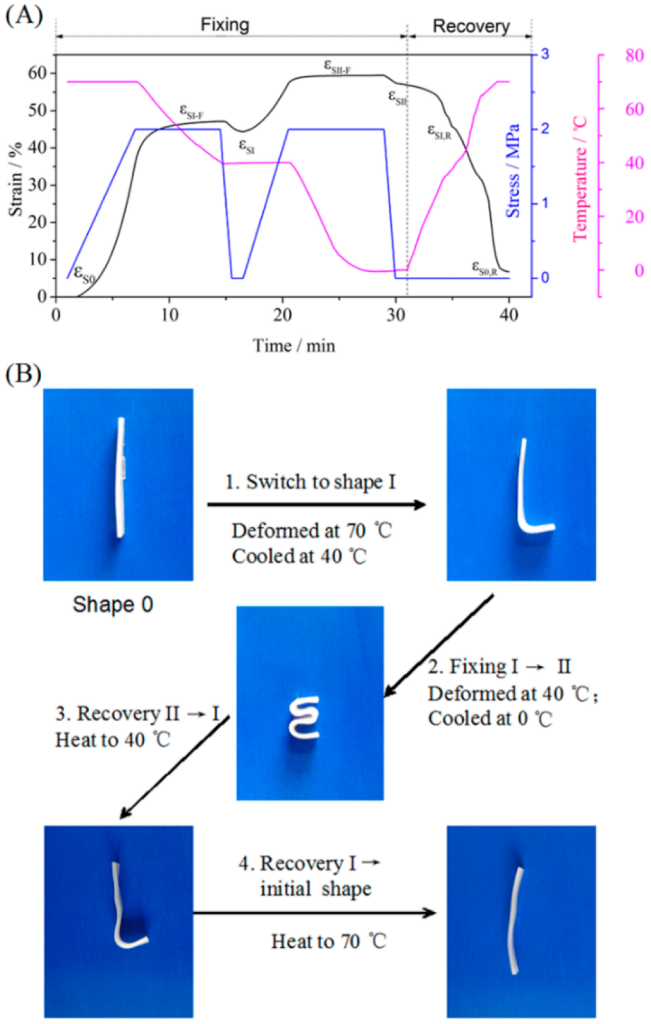


**Figure 4.** (A) Quantitative demonstration of triple shape memory properties of TSMPU with DMA; (B) qualitative process of triple shape memory fixing and recover.

segments and the crosslinked structure of hard segments are acted as two transition regions, which result in the thermal-induced triple shape memory effect. The molecular chain states in each process of shape memory effect are shown in Scheme 2. When the polymer is heated to 70 °C, the crystalline region will be melted, and thus all segments have a good motion performance. When the polymer is cooled to 40 °C, the hard segment with the crosslinking network will be frozen slowly, whereas the PCL-diols chains are still motived, corresponding to the stage that the initial shape was fixed to the shape I. In this stage, only the crosslinking structure acts as the reversible phase, and the rest of hard segments of TSMPU act as the fixed phase. When the polymer is placed in ice water, the movement of all molecular chains is restrained, corresponding to the stage that the shape I was fixed to the shape II. The hard segments and soft segments work as the fixed phase and the reversible phase, respectively. Importantly, in the shape recovery process, the shape II recovers to the shape I, then to the initial shape, the cross-linked structure and soft segments have the same role as the shape-fixed process.[44]

**Mechanical Properties of TSMPU.** Important to their performance in biomedical applications, the mechanical properties of the TSMPU(s) were investigated. Figure 5 shows the stress−strain curves of the TSMPU with different

**Scheme 2. Mechanism of Triple Shape Memory Effect of TSMPU.**

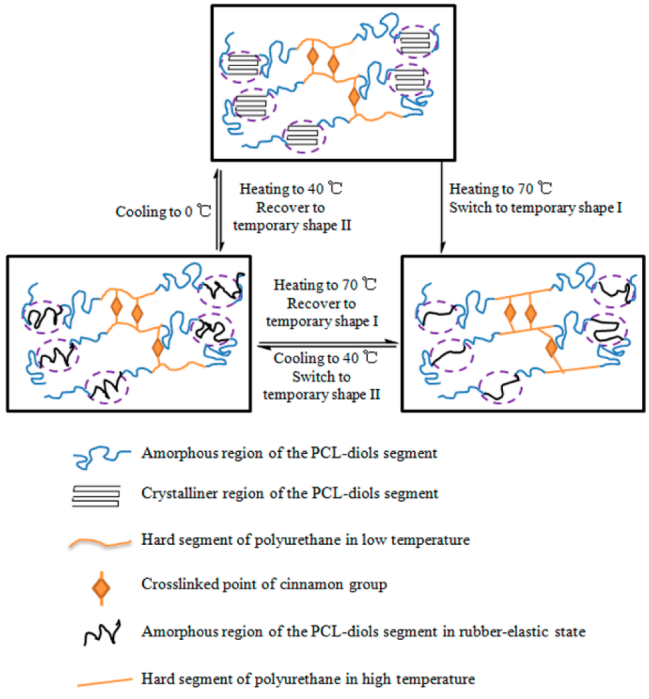


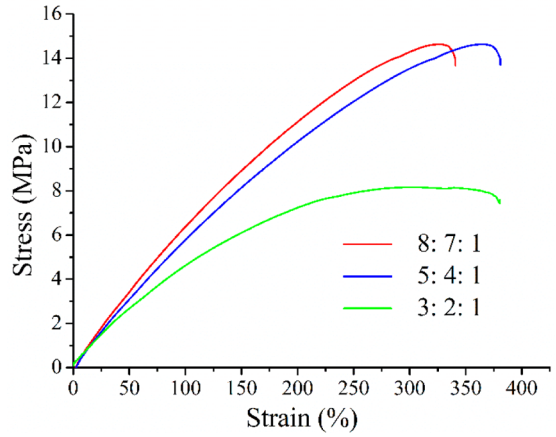


**Figure 5.** Stress−stain curves of PCLU with different ratios of hard segment.

ratios of hard segments and soft segments. The result displays a typical thermoplastic mechanical property of polymer. The elongation at break decreases, however, the maximum tensile strength ($\varepsilon_m$) increases from 8.1 MPa to 13.0 MPa, and 15.2 MPa for PCLU with MDI : BHECA : PCL ratio of 3:2:1 increasing to 5:4:1, 8:7:1, respectively. With the increase of the soft segments (PCL segments), the elongation at break increases and $\varepsilon_m$ decreases. The mechanical properties are mainly dependent on the proportion of the soft segments and the hard segments in the copolymer. Then the elongation at break increases and $\varepsilon_m$ decreases with the increase in the soft segments.

The tensile modulus ($E$) of TSMPU increases from 5.01 MPa to 6.42 MPa and 7.26 MPa with the increasing of hard segments. The increase is likely due to the increasing of the crosslinking structure formed by cinnamon groups in hard


dx.doi.org/10.1021/am402091m | ACS Appl. Mater. Interfaces 2013, 5, 10520−10528

segments. The volumetric cross-link density ($n$) is calculated by the following equation[45]

$$n = \frac{E}{3RT} \quad (7)$$

Where $E$ is the tensile modulus, $R$ is the gas constant, and $T$ is the temperature (Table 2). In Table 2, we can find that the volumetric crosslink density of TSMPU increases with the increase of the hard segments because the cinnamon groups increase in the hard segments.

**Cytotoxicity Analysis.** It is essential that a biomaterial used for an implantable device be noncytotoxic. Osteoblasts cells are cultured to evaluate the cytotoxicity of the synthesized TSMPU based on Alamar blue assay. The cytotoxicity of TSMPU (3:2:1), TSMPU (5:4:1) and TSMPU (8:7:1) was assessed by detecting the absorbance at 570 nm in Alamar blue assay. From Figure 6A, we can find that the polymers exhibit high cell viability for culture of 3 days and 5 days, indicating its better non-cytotoxicity. To further confirm the non-cytotoxicity of TSMPU, the morphology of osteoblasts is observed by optical microscopy as shown in Figure 6B. It can be clearly found that the osteoblasts grew healthily and attached well on the all TSMPU films. The results suggest that the polymers possess good noncytotoxicity, and are potentially suitable for the application of biomaterials.

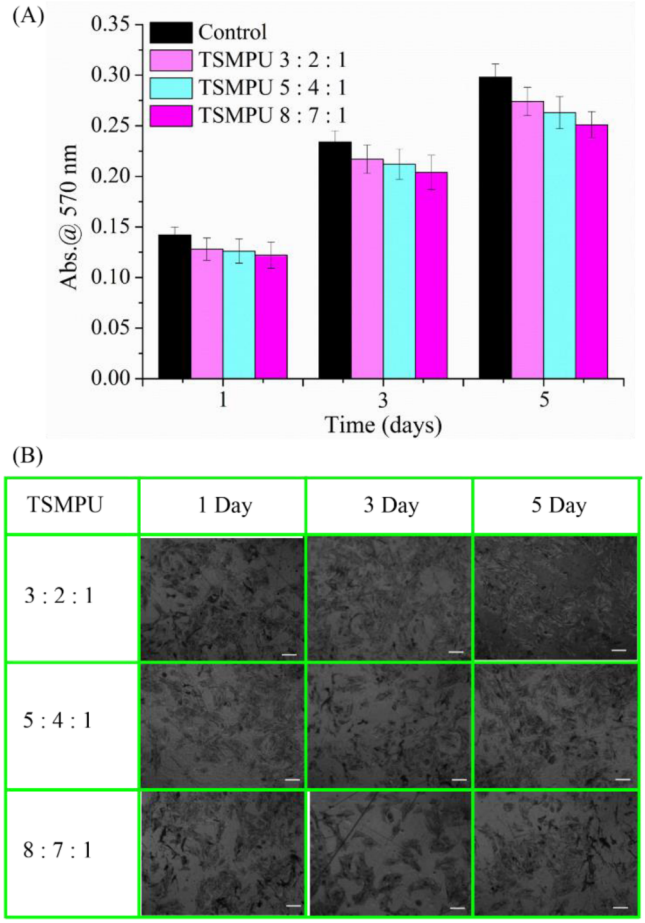


**Figure 6.** (A) Alamar blue analysis and (B) optical microscope images of osteoblasts cultured on TSMPU films with different ratios of hard segment at day 1, 3, and 5, respectively. All the scale bars represent 50 $\mu$m.

## CONCLUSIONS

In summary, we obtained a new triple shape memory system with pendant cinnamon groups, which includes both a $T_m$-type segment and a $T_g$-type segment through a photo-crosslinking. The chemical structure was confirmed by FT-IR, $^1$H NMR, and UV−vis. The DSC and DMA results demonstrated that the TSMPU had two transition temperatures, of which one is the melting point of PCL-diols from the polyurethane soft segment, and the other is the cross-linked structure of the polyurethane hard segment. These polymers have good thermal-induced triple shape memory effect, and the $T_{trans}$ can be adjusted to the temperature close to the body temperature by altering the ratio of the soft and hard segments. Alamar blue analysis exhibits that the polymers possess good noncytotoxicity. Therefore, these results indicate that the TSMPU possess a great potential for use in biomedicine devices.

## ASSOCIATED CONTENT

### Supporting Information

$^1$H NMR spectrum of methyl cinnamate. The SEM and AFM images of the cross-section with freeze-fracture and the film surface of PCLU and TSMPU. The movie showing the triple-shape memory process. The shape fixity ratio and shape recovery ratio for TSMPU (5:4:1) with three times. This material is available free of charge via the Internet at http://pubs.acs.org.

## AUTHOR INFORMATION

### Corresponding Author

*E-mail: shaobingzhou@hotmail.com or shaobingzhou@swjtu.cn. Fax: 86-28-87634649. Tel: 86-28-87634068

### Notes

The authors declare no competing financial interest.

## ACKNOWLEDGMENTS

This work was partially supported by National Basic Research Program of China (973 Program, 2012CB933600), National Natural Science Foundation of China (30970723, 51173150, 51373138), Research Fund for the Doctoral Program of Higher Education of China (20120184110029), and Fundamental Research Funds for The Central Universities (SWJTU11ZT10).

## REFERENCES

(1) Behl, M.; Lendlein, A. *Mater. Today* **2007**, *10*, 20−28.
(2) Behl, M.; Razzaq, M. Y.; Lendlein, A. *Adv. Mater.* **2010**, *22*, 3388−3410.
(3) Garle, A.; Kong, S.; Ojha, U.; Budhlall, B. M. *ACS Appl. Mater. Interfaces* **2012**, *4*, 645−657.
(4) Guo, W.; Kang, H.; Chen, Y.; Guo, B.; Zhang, L. *ACS Appl. Mater. Interfaces* **2012**, *4*, 4006−4014.
(5) Fan, M. M.; Yu, Z. J.; Luo, H. Y.; Zhang, S.; Li, B. J. *Macromol. Rapid. Comm.* **2009**, *30*, 897−903.
(6) Zheng, X.; Zhou, S.; Li, X.; Weng, J. *Biomaterials* **2006**, *27*, 4288−4295.
(7) Lendlein, A.; Jiang, H.; Jünger, O.; Langer, R. *Nature* **2005**, *434*, 879−882.
(8) Mayer, G.; Heckel, A. *Angew. Chem., Int. Ed.* **2006**, *45*, 4900−4921.
(9) Xiao, Y.; Zhou, S.; Wang, L.; Gong, T. *ACS Appl. Mater. Interfaces* **2010**, *2*, 3506−3514.
(10) Mohr, R.; Kratz, K.; Weigel, T.; Lucka-Gabor, M.; Moneke, M.; Lendlein, A. *Proc. Natl. Acad. Sci. U.S.A.* **2006**, *103*, 3540−3545.
(11) Du, H.; Zhang, J. *Soft Matter* **2010**, *6*, 3370−3376.

(12) Ratna, D.; Karger-Kocsis, J. *J. Mater. Sci.* **2008**, *43*, 254−269.
(13) Ward Small, I. V.; Singhal, P.; Wilson, T. S.; Maitland, D. J. *J. Mater. Chem.* **2010**, *20*, 3356−3366.
(14) Lendlein, A.; Behl, M.; Hiebl, B.; Wischke, C. *Expert Rev. Med. Devices* **2010**, *7*, 357−379.
(15) Xue, L.; Dai, S.; Li, Z. *Biomaterials* **2010**, *31*, 8132−8140.
(16) Guignot, C.; Betz, N.; Legendre, B.; Le Moel, A.; Yagoubi, N. *Nucl. Instrum. Methods Phys. Res., Sect. B* **2001**, *185*, 100−107.
(17) Li, J.; Xie, T. *Macromolecules* **2010**, *44*, 175−180.
(18) Zhao, J.; Chen, M.; Wang, X. Y.; Wang, Zh.; Dang, Zh.; Ma, L.; Hu, G. H.; Chen, F. H. *ACS Appl. Mater. Interfaces* **2013**, *5*, 5550−5556.
(19) Shao, Y.; Lavigueur, C.; Zhu, X. X. *Macromolecules* **2012**, *45*, 1924−1930.
(20) Zotzmann, J.; Behl, M.; Feng, Y.; Lendlein, A. *Adv. Funct. Mater.* **2010**, *20*, 3583−3594.
(21) Xie, T. *Nature* **2010**, *464*, 267−270.
(22) Zhang, Q.; Song, S.; Feng, J. *J. Mater. Chem.* **2012**, *22*, 24776−24782.
(23) Lendlein, A.; Behl, M. *Adv. Sci. Technol.* **2009**, *54*, 96−102.
(24) Bellin, I.; Kelch, S.; Langer, R.; Lendlein, A. *Proc. Natl. Acad. Sci. U.S.A.* **2006**, *103*, 18043−18047.
(25) Yakacki, C. M.; Gall, K. *Adv. Polym. Sci.* **2010**, *226*, 147−175.
(26) Hoskins, J. N.; Grayson, S. M. *Macromolecules* **2009**, *42*, 6406−6413.
(27) Behl, M.; Ridder, U.; Feng, Y.; Kelch, S.; Lendlein, A. *Soft Matter* **2009**, *5*, 676−684.
(28) Lee, B. S.; Chun, B. C.; Chung, Y. C.; Sul, K. I.; Cho, J. W. *Macromolecules* **2001**, *34*, 6431−6437.
(29) Ping, P.; Wang, W.; Chen, X.; Jing, X. *Biomacromolecules* **2005**, *6*, 587−592.
(30) Wang, W.; Ping, P.; Yu, H.; Chen, X.; Jing, X. *J. Polym. Sci., A: Polym. Chem.* **2006**, *44*, 5505−5512.
(31) Xue, L.; Dai, S.; Li, Z. *Macromolecules* **2009**, *42*, 964−972.
(32) Wu, L.; Jin, C.; Sun, X. *Biomacromolecules* **2010**, *12*, 235−241.
(33) Zhou, S.; Deng, X.; Yang, H. *Biomaterials* **2003**, *24*, 3563−3570.
(34) Jin, C.; Sun, X.; Wu, L. *Des. Monomers. Polym.* **2011**, *14*, 47−55.
(35) Narasimhan, B.; Belsare, D.; Pharande, D.; Mourya, V.; Dhake, A. *Eur. J. Med. Chem.* **2004**, *39*, 827−834.
(36) Shao, S.; Zhou, S.; Li, L.; Li, J.; Luo, C.; Wang, J.; Li, X.; Weng, J. *Biomaterials* **2011**, *32*, 2821−2833.
(37) Ahmad, M.; Luo, J.; Xu, B.; Purnawali, H.; King, P. J.; Chalker, P. R.; Fu, Y.; Huang, W.; Miraftab, M. *Macromol. Chem. Phys.* **2011**, *212*, 592−602.
(38) Luo, X.; Mather, P. T. *Adv. Funct. Mater.* **2010**, *20*, 2649−2656.
(39) Cuevas, J. M.; Rubio, R.; Germán, L.; Laza, J. M.; Vilas, J. L.; Rodriguez, M.; M. León, L. *Soft Matter* **2012**, *8*, 4928−4935.
(40) Ping, P.; Wang, W.; Chen, X.; Jing, X. *J. Polym. Sci. B: Polym. Phys.* **2007**, *45*, 557−570.
(41) Kim, B. K.; Lee, S. Y.; Xu, M. *Polymer* **1996**, *37*, 5781−5793.
(42) Saralegi, A.; Rueda, L.; Fernandez Arlas, B.; Mondragon, I.; Eceiza, A.; Corcuera, M. A. *Polym. Int.* **2013**, *62*, 106−115.
(43) Kloss, J.; Munaro, M.; De Souza, G. P.; Gulmine, J. V.; Wang, S. H.; Zawadzki, S.; Akcelrud, L. *J. Polym. Sci. B: Polym. Chem.* **2002**, *40*, 4117−4130.
(44) Sun, L.; Huang, W. *Soft Matter* **2010**, *6*, 4403−4406.
(45) Wang, Y.; Ameer, G. A.; Sheppard, B. J.; Langer, R. *Nat. Biotechnol.* **2002**, *20*, 602−606.